Detection and reconstruction of short-lived particles produced by neutrino interactions in emulsion

Uiterwijk, J.W.H.M.

Chapter 5

Measurement of D^{*+} production

In this chapter, a result published by the CHORUS collaboration [256] is presented. The large amount of emulsion exposed to the high-intensity ν_μ beam at CERN makes it possible to study charm-meson production and decay with relatively high statistics and excellent resolution. About 100,000 charged-current ν_μ interactions have been found in the emulsion. Among these events, charmed-meson decays have been identified from the presence of a secondary vertex. Part of these charmed mesons are produced as a D^{*+} resonance, which immediately decays strongly to a pion and a D meson. In the CHORUS experiment, one can identify a D^0 meson from its decay in the emulsion and charged pions can be indentified and measured in the hadron spectrometer. Hence, a measurement of the D^{*+} production cross-section can be made.

The measurement relies on an accurate determination of the charge and momentum of pions. Therefore, the upgrade of the hadron spectrometer with the honeycomb detector, described in Chapter 3, played an important role in this measurement. The techniques to find and reconstruct events in the emulsion have been discussed in Chapter 2. The exact layout of the emulsion stacks can also be found in that chapter. Possible upgrades to the event location and reconstruction techniques, although not used for this measurement, have been given in Chapter 4.

In this chapter, the phenomenology of charmed-meson production in neutrino interactions is given first. The experimental procedure to extract charmed-meson decays in the emulsion is described next, followed by the selection of events due to D^{*+} decays. After a discussion of the background and selection efficiency derived from a Monte-Carlo simulation, the number of D^{*+} events is given. From this number, the ratio of charmed vector meson (D^*) to scalar meson production (D^+,D^0) and the D^{*+} production cross-section with respect to the total charged-current ν_μ cross-section are derived.

5.1 Introduction

The measurement of the D^{*+} production cross-section and the comparison with the total D^0 production cross-section give some insight into the charm-production mechanism. In particular, the ratio of charmed vector meson and scalar meson production in deep-inelastic scattering can be obtained. Several experimental groups have performed a study of D^{*+} production in neutrino charged-current interactions [257–259]. In these experiments the identification of charmed particles relied mainly on the reconstruction of the invariant mass of the assumed decay products.

In emulsion experiments, charm production can be observed without the need to reconstruct the invariant mass. The tracking in emulsion has enough spatial resolution to clearly separate the charm-decay vertex from the primary neutrino-interaction vertex. In hybrid experiments, combining the emulsion technique with electronic detectors, the high spatial resolution at the neutrino and decay vertices can be combined with kinematical measurements of the outgoing particles. This technique has been applied in a neutrino beam by the E531 experiment at FNAL. However, the number of events accumulated in the 25 kg of emulsion was limited.

Recent improvements in automatic emulsion scanning systems made it possible to measure several orders of magnitude larger volumes of emulsion. In the CHORUS experiment, the high intensity neutrino beam from the CERN SPS (section 2.2) was used in conjuction with an 800 kg emulsion target. The net-scan technique was used to examine a large volume of emulsion around neutrino interactions and a high statistics sample of charm decays has been collected.

Contrary to the previous experiments which use the reaction $D^{*+} \to D^0 \pi^+$ to tag the D^0, in the CHORUS experiment the D^0 is directly recognized by its decay topology, independently of the presence of the D^{*+} parent. Therefore, the D^{*+} sample is obtained through the recognition of the above reaction as a subset of an already very pure sample of D^0 events. This offers the unique opportunity to measure the D^{*+} production rate relative to the D^0 production cross-section without the need for an external normalization.

5.2 Charm-quark production and fragmentation

An extensive description of the theory of charm-quark production and fragmentation and a discussion of the previous experimental results can be found in Ref. 215. Here a brief overview of the phenomenology of charm-quark production and fragmentation is given.

The theoretical description of neutrino–nucleon scattering is rather complex because the nucleon is not an elementary point-like particle. The complexity arises, not from the theoretically well-understood weak interaction, but from the substructure of the nucleon and from nucleon–nucleon interactions inside a nucleus. The scattering cross-section is normally described in terms of structure functions which describe the internal structure of the nucleon. The structure functions represent quark and gluon-density distributions inside a nucleon.

The interactions between quarks and gluons is described by a theory known as quantum-chromo-dynamics (QCD). It is a non-Abelian gauge theory which means that the force-carrying bosons, the gluons, carry colour charges themselves. Because the glu-

ons have colour charges, they can interact with each-other, a process which is thought to be responsible for the confinement of quarks in colour-neutral hadrons. In interactions with high four-momentum transfer, the quark masses can usually be neglected, and the structure functions and cross-sections for these processes can be calculated using perturbation theory. On the contrary, in charm production and at the typical four-momentum transfer $Q^2 = 10\,\mathrm{GeV}^2/\mathrm{c}^2$ for the CHORUS experiment, the mass of the charm quark $m_c \approx 1.5\,\mathrm{GeV}/c^2$ can no longer be neglected. As the charm-quark mass is similar to the nucleon mass, one can also no longer neglect the nucleon mass in the cross-section calculations.

Charged-current neutrino interactions are mediated by $W^{\pm}$ bosons and are sensitive to the quark-flavour distributions. Neutrino–nucleon scattering is therefore an essential tool in determining the individual quark-density functions and related structure functions. As a case in hand, charm production by neutrino–nucleon interactions is especially sensitive to the strange-sea distribution in the nucleon. Even though the down valence-quark distribution is about 10 times bigger in a proton, the $d \to c$ transition is Cabibbo suppressed. As a result, the $d \to c$ and $s \to c$ processes give about equal contributions to the cross-section. The diagrams for these processes are given in Figure 5.1. From the difference of the charged-current neutrino and anti-neutrino scattering cross-sections with a charmed quark in the final state, one can extract the valence down-quark density function. The quark and anti-quark contributions from the down and strange sea are expected to be equal and cancel in the difference.

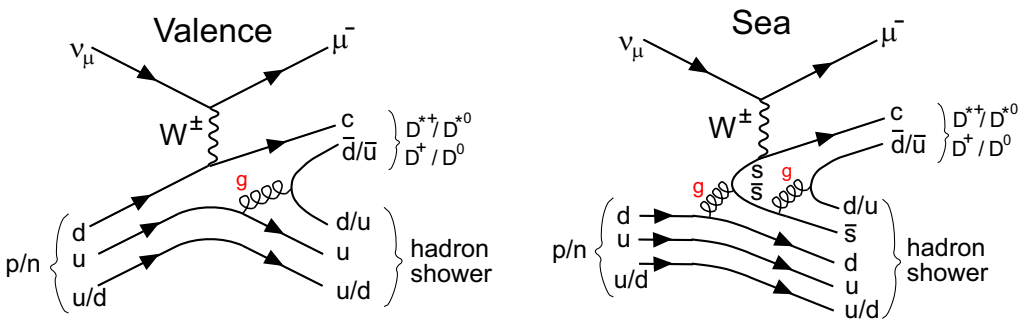

Figure 5.1: Schematic diagrams of charmed meson production by neutrino–nucleon interactions. The valence diagram is Cabibbo suppressed. The sea contribution, indicated by a gluon splitting in an $s\bar{s}$ pair, is Cabibbo favoured and similar to the valence contribution at the typical energies in CHORUS.

After the production of a charm quark, one still has to understand how the charm quark ends up in the hadronic final state. This process is known as hadronization or fragmentation. From the number of available spin states, one expects to produce three times as many vector mesons than pseudo-scalar mesons. In the case of charm production, the vector mesons are the D^{*+} and the D^{*0}; the pseudo-scalar mesons are the D^+ and the D^0. Furthermore, under isospin invariance and assuming similar mass for the up and down quark, the probability that the charm quark combines with an anti-up or anti-down quark is equal. The production cross-sections for D^0 and D^+ (D^{*+} and D^{*0}) are therefore equal. The D^{*0} resonance decays strongly to $D^0\,\pi^0$ or electro-magnetically to $D^0\,\gamma$, because the decay to $D^+\,\pi^-$ is energetically forbidden. The D^{*+} resonance decays for about 2/3 to $D^0\,\pi^+$ and for about 1/3 to $D^+\,\pi^0$. One then finds that the expected

production ratio of D^+ to D^0 in the final state is 1:3. This fragmentation is schematically indicated on the right-hand side of the diagrams of Figure 5.1.

One should remember that in an experiment only some quantities of the final state are accessible. In neutrino experiment at a wide-spectrum neutrino beam, not even the initial state is known. However, in CHORUS the final-state muon momentum and the total hadronic energy is measured. In a charged-current ν_μ interaction, these two variables do determine the initial neutrino momentum.

Most charm-production cross-section measurements in neutrino experiments rely on the muonic decay of the charmed hadrons, as the individual charm particles cannot be identified due to their short flight length. These events, known as dimuon events, are characterized by two opposite-sign muons in the detector coming from the same initial vertex. Experiments based on this signature basically group all charmed hadrons for which an average charm to muon branching ration, $B_{c\to\mu}$, is observed. This average branching ratio is given by the sum over all types of charmed hadrons

$$B_{c\to\mu} = \sum_t f_{h_t} \cdot B(h_t \to \mu) \quad ,$$

where f_{h_t} is defined as the probability that a charmed quark hadronizes into a charmed hadron h_t, with the obvious normalization $\sum_t f_{h_t} = 1$. The semi-leptonic branching ratios entering into the definition of $B_{c\to\mu}$ have been determined to a reasonable degree of accuracy in e^+e^- experiments, both at the $c\bar{c}$ threshold and at higher energies. Unfortunately, this is not true for the production fractions f_{h_t}. Furthermore, f_{h_t} depends on energy, mostly due to the energy dependence of the Λ_c^+ production cross-section.

By their very nature, the f_{h_t} can only be measured in those neutrino experiments that are capable of identifying the charmed hadron. So far, only the E531 experiment [202] has conducted such an experiment. To tag and identify charmed particles produced in neutrino interactions, it used an emulsion target followed by a series of electronic detectors providing both kinematic reconstruction and particle identification. From a study of 122 charmed-particle decays among 3855 located neutrino interactions, the E531 collaboration has extracted the production fraction for each of the charmed hadrons [260]. The experiment also measured the dependence on the kinematic variables [261]. This sample of 122 events continues to be the only reference for the production fractions f_{h_t} and has been reanalyzed in Ref. 262. The results of all dimuon experiments rely heavily on this single measurement.

The E531 experiment was set up specially for charm physics studies, CHORUS on the other hand has many more events in the emulsion but is unable to reliably identify the type of charmed hadron because it has no particle-identification detectors and lacks accuracy in the hadron spectrometer. However, CHORUS can perfectly distinguish charged charmed hadrons from neutral ones and can make a sample selection that is essentially background free. Statistically, the f_{h_t} fractions can be extracted from the distributions of flight length and energies. On an event by event basis, a particle-identification probability can be assigned from the flight length and decay topology measured in the emulsion.

The charm detection in CHORUS relies on the net-scan technique. The primary neutrino vertex in a ν_μ charged-current interaction can be efficiently located by tracking back the muon through the emulsion plates. With the net-scan technique, all tracks (up to 5 mm) downstream from the neutrino vertex can be reconstructed and secondary vertices extracted. Secondary vertices with even numbers of tracks and no nuclear remnant

tracks, can only be due to decays of short-lived neutral particles. At the energy scale of CHORUS, only the D^0 contributes to this signal. Secondary vertices with an incoming track connected to the primary vertex, an odd number of outgoing tracks, and again no interaction are most likely from $D^{\pm}$ decays.

5.3 Vertex reconstruction and charm sample selection

As was described in section 2.8, tracks found in the target tracker are used to predict the position of neutrino interactions in the emulsion. In particular, for charged-current ν_μ interactions, the primary muon is used to predict with high precision the point where it traversed the changeable sheets. The muon is identified by its range in the calorimeter and the muon spectrometer. The layout of the emulsion target and trackers is described in section 2.4. The approximate neutrino interaction point is located by following the prediction upstream from plate to plate in the scan-back procedure. In order to select charm-decay candidates, the net-scan procedure is used to reconstruct all high-energy tracks originating in a 1.5 mm × 1.5 mm × 6.3 mm volume around the located neutrino interaction. The scan-back and net-scan procedures are explained in section 2.10. As is described there, in the net-scan procedure tracks are connected over multiple plates and only tracks originating from witin the net-scan volume are kept. The reconstruction algorithm then tries to associate those tracks to common vertices. A track is attached to a vertex if the distance of the vertex point to the reconstructed track (referred to as the impact parameter) is less than 10 μm. At the end of the vertex-assignment procedure, one defines a primary vertex and possibly one or more secondary vertices. In the following, tracks origination from secondary vertices are called daughter tracks.

Candidate events for ν_μ charged-current interactions with a charm decay are then automatically selected from the set of reconstructed events. An event is defined as a candidate for a charged-current ν_μ interaction if the primary muon track, identified in the electronic detectors, is connected to the neutrino-interaction vertex and is found in more than one emulsion plate in the net-scan data. Decay topologies are then selected with the following criteria. At least one of the tracks connected to a secondary vertex is detected in more than one plate and the direction measured in the emulsion matches that of a track reconstructed in the target trackers. The parent angle, in the case of a neutral particle decay deduced from the line connecting the primary and secondary vertex, should be within 400 mrad from the beam direction. To avoid including too many fake secondary vertices due to multiple scattering of low-energy tracks from the primary vertex, the impact parameter to the primary vertex of at least one of the daughter tracks must be larger than a certain value which is determined on the basis of the angular resolution. The angular resolution depends on the track angle (θ) with respect to the beam as $\sigma_\theta(\theta) = \sqrt{3^2 + (19.4 \cdot \tan\theta)^2}$ mrad. In order to remove random association, the impact parameter is also required to be smaller than a value depending on the distance covered by the track extrapolation to the vertex. The typical tolerance is 130 μm. The flight length of the parent candidate should be longer than 25 μm.

Out of a sample of 93,807 scanned and analysed neutrino-induced charged-current events, these criteria select 2752 events as having a decay topology. The automatic scanning only measures the most upstream 100 μm parts of the tracks on successive emulsion plates. It, therefore, does not see the actual vertices and can, for example, not distinguish between a neutral or charged short-lived particle if it does not cross a plate

boundary. Nor can it distinguish between decay and interaction vertices. Therefore, the selected events are visually inspected to confirm the presence of a decay. A secondary vertex is accepted as a decay if the number of charged particles is consistent with charge conservation. In addition, no other activity (Auger-electron or visible recoil) should be observed. In this analysis, only those events are used in which the secondary vertex is consistent with the decay of a neutral particle. Thus the selection and identification of the D^0 sample used in this analysis is based on the decay topology of the D^0 alone.

Decay candidates are selected from all charged-current events:

Located charged-current events	93,807
Selected for visual inspection	2752

Visual inspection of the decay candidates rejected 739 events because:

Decay topologies with flight length $< 25\,\mu$m	3
Topologies with kink angle < 50 mrad	11
Secondary interactions	278
Electron–positron pairs	95
Overlay neutrino interactions	44
Uncorrelated (overlay) secondary vertices	21
Passing-through tracks	128
All tracks from primary vertex	142
δ-rays	2
Other	15
Total rejected by visual inspection	739

The remainder are charm-decay candidates with the following signatures:

Charged charm: 1-prong decay (kink)	452
Charged charm: 3-prong decay	491
Charged charm: 5-prong decay	22
Neutral charm : 2-prong decay vertex (V2)	819
Neutral charm : 4-prong decay vertex (V4)	226
Neutral charm : 6-prong decay vertex (V6)	3
Total charm candidates	2013

Table 5.1: Number of located and reconstructed events in the emulsion from the charged-current data sample and the charm sub-sample.

The results of the visual inspection are summarized in Table 5.1. The purity of the automatic selection is $[73.1 \pm 0.8]\,\%$. The rejected sample consists of secondary hadronic interactions, δ-rays or gamma conversions, overlay neutrino interactions, and of low-momentum tracks which, due to multiple scattering, appear as tracks with a large impact parameter. The remainder consists either of false vertices, being reconstructed using one or more background tracks, or of vertices with a parent track not connected to the primary (passing-through tracks).

5.4 Event selection of $D^{*+} \to D^0 \pi^+$

The identification of D^{*+} is based on its decay into D^0 and π^+:

$$D^{*+} \to D^0 \pi^+ \quad . \tag{5.1}$$

The reconstruction of the invariant mass of the D^{*+} would require to measure momenta of at least three charged hadrons, namely the π^+ from the D^{*+} decay and two charged decay daughters of the D^0 for the most favourable decay mode, $D^0 \to K^- \pi^+$ with a branching ratio of $[3.80 \pm 0.09]\,\%$. Such a strategy would result in a very small event-selection efficiency and has therefore not been applied.

The procedure applied here relies on the high purity of the sample of D^0 events identified by the decay topology in emulsion and by the low Q-value of the D^{*+} decay. The Q-value corresponds to a maximum p_T of $39\,\mathrm{MeV}/c$). The π^+ from the D^{*+} decay has a relatively low momentum ($< 4\,\mathrm{GeV}/c$) and, as a consequence of the low Q-value, a small angle with respect to the D^0 direction. In this two-body decay, the transverse momentum spectrum of the π^+ with respect to the D^0 direction shows a Jacobian peak below $40\,\mathrm{MeV}/c$. The kinematical quantities needed for this approach are the direction of the π^+, the momentum of the positive pion, and the direction of the D^0.

5.4.1 D^0 secondary vertex selection

The selection starts from the sample of D^0 events, characterized by the decay topology into two or four charged particles as is described above and in Ref. 263. In total, the sample contains 1048 D^0 events of which 1045 decayed into two and four prong modes. For each particle track, recognized in the emulsion as originating from the primary vertex, a charge selection is made and the transverse momentum, p_T, with respect to the direction of the D^0 is measured.

In the CHORUS experiment, the track reconstruction in the emulsion target determines the slope of the charged particles with high precision (order 1 mrad). The direction of the D^0 is determined from the measurement of the positions of the primary neutrino interaction vertex and the decay vertex. The precision of this determination depends on the decay length. For this measurement of the D^{*+} cross-section, only decays with a flight length of more than $100\,\mu$m are used to ensure good resolution.

5.4.2 Primary π^+ selection

The momentum measurement of the particles reconstructed in the emulsion is performed by extrapolating the tracks from the emulsion to the target tracker and to the hadron spectrometer (section 2.6.1). In order to select the tracks with a reliable momentum determination, strict requirements are applied on the measurements in the hadron spectrometer. Only tracks with a hit in all six paddles of the diamond tracker or with track segments in the honeycomb tracker (Chapter 3) and a smaller number of hits in the diamond tracker were retained. The 488 selected events with a D^0 (see section 5.4.4), had 1116 hadron tracks reconstructed at the primary vertex. Of these, the momentum of 377 particles was measured fullfilled the criteria just given. The inefficiency can be attributed in about equal parts to secondary interactions in the target material and to the limited geometrical acceptance of the hadron spectrometer. The resolution of the hadron spectrometer is about 35 % for the low momentum range relevant for this study.

5.4.3 Monte-Carlo simulation

In order to study the potential separation power between signal and background, the p_T distribution was studied using a simulation of the events originating in the four stacks of the emulsion target separately. Figure 5.2 shows the p_T distribution of the simulated D^0 candidates (including events where the D^0 was produced from the decay of the D^{*+}), selected by the same selection criteria as used for the data. The solid curve is the prediction for combinations of D^0's with positively-charged hadrons including the expected signal. The dashed curve is the sample of D^0's which do not originate from the reaction $D^{*+} \rightarrow D^0 \pi^+$. The data for the four stacks are based on the same simulated sample and thus predict the relative weight of the signal to be observed in the four stacks. A good separation between signal and background is possible only for interactions originating in the two downstream stacks (stack 3 and 4). Therefore, only the events originating in these two stacks were considered in the analysis. The signal-to-background ratio is most favourable in the p_T region from 10 MeV/c to 50 MeV/c. This region is used as signal region in the analysis.

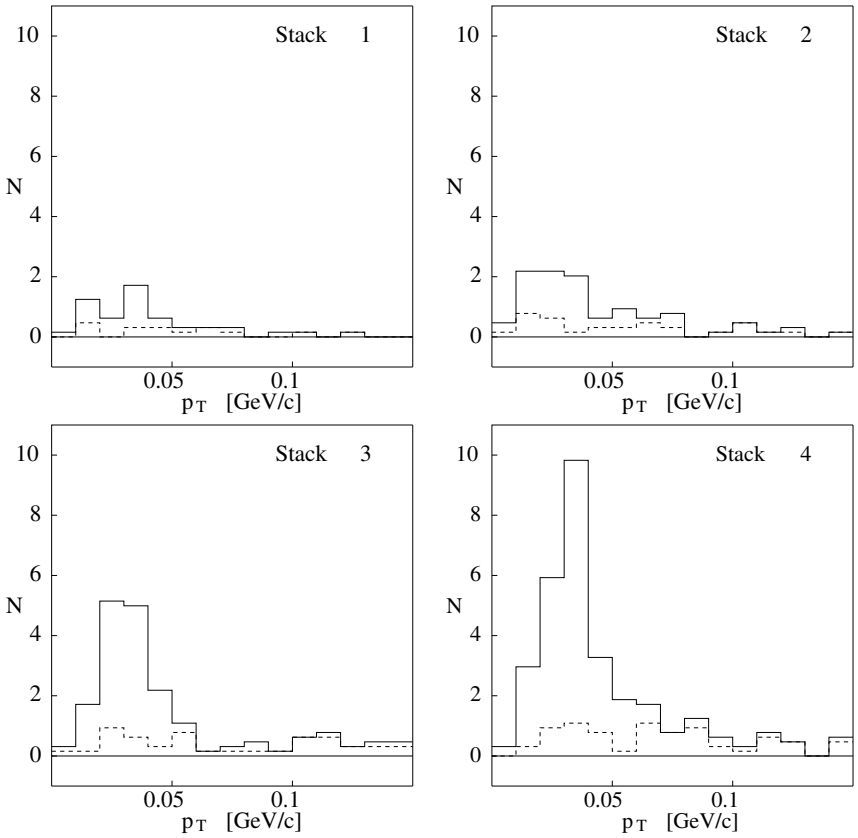

Figure 5.2: Number of charged hadrons (N) from the primary vertex as a function of the transverse-momentum (p_T) with respect to the D^0 direction as obtained from a simulation. The four panels show the results of the simulation for the four emulsion stacks, stack 1 being the most upstream stack. For an explanation of the curves see the main text.

The loss of efficiency and signal-to-noise ratio for the upstream stacks are easy to understand. They are the result of the low average momentum ($\approx 1\,\mathrm{GeV}/c$) of the π^+ in reaction (5.1). Multiple scattering plays a large role together with re-interactions in the downstream stacks. Therefore the matching of the track seen in the emulsion with the hits in the hadron spectrometer has a low efficiency when a large amount of material has been traversed by the particle.

5.4.4 Signal extraction

The candidate events were searched within the sample of 488 D^0 events in stacks 3 and 4 with a D^0 flight length l_f exceeding $100\,\mu$m. After removing tracks identified as muons, 1116 tracks originating from the primary vertex were found in these events. To obtain an enriched sample of candidate events within this sample, the following set of kinematical criteria was applied. Since the typical momentum of the π^+ from D^{*+} decay is smaller than $4\,\mathrm{GeV}/c$, hadrons with a momentum greater than this value were not considered. In addition, tracks having a measured momentum smaller than $400\,\mathrm{MeV}/c$ were rejected. These tracks are more likely to come from secondary hadrons and from random coincidences of hits in the tracking system of the hadron spectrometer. The angle between the hadron and the D^0 was required to be smaller than 60 mrad. The simulation showed that the signal does not populate the region with larger angles. For the remaining tracks, a separation between positive and negative charges was made and the p_T spectra were further analysed. The result of the event and track selection is given in Table 5.2.

Number of events with secondary D^0 and associated hadron tracks:

Stacks:	1 and 2	3 and 4
Visually confirmed D^0 decays	521	527
D^0 decays selected for analysis ($l_f \geq 100\,\mu$m)		488
Hadron tracks at the primary vertex		1116
Hadrons from primary vertex with measured p		377

Selection of known-momentum hadron tracks in $D^{*+} \to D^0\,\pi^+$ signal region:

Charge:	positive	negative
Hadrons from primary vertex with measured p	248	129
Within angular range ($\theta(\pi, D^0) < 60\,\mathrm{mrad}$)	62	26
Within momentum window ($0.4 < p < 4\,\mathrm{GeV}/c$)	47	12
In p_T signal region ($10 < p_T < 50\,\mathrm{MeV}/c$)	27	4

Table 5.2: Number of events and tracks used in the analysis.

Figure 5.3 shows the p_T distributions of positively charged hadrons and negatively charged hadrons originating from the primary vertex in the D^0 data sample and in a sample of charged-charm production events. In the figure, the points with error bars show the number of candidate events with the statistical error. The dashed curve shows the background prediction. In the distribution for the D^0 with positive hadrons, the solid

curve represents the expected shape of the candidate events (including the background simulation) normalized to the observed events. In the other panels, the solid curve shows the prediction for the shape normalized to the total number of D^0's and charged charm events, respectively. An excess which can be attributed to the signal is visible in the range between $10\,\mathrm{MeV}/c$ to $50\,\mathrm{MeV}/c$ in the p_T distribution of positive hadrons in the D^0 sample, while in the p_T distribution of negative hadrons no such excess is seen. In addition, if one makes the same comparison between the p_T spectra of positive and negative hadrons with respect to charged charm particles found in the same stacks and with the same kinematical cuts, no such signal can be seen. This behaviour is a clear indication of D^{*+} decays.

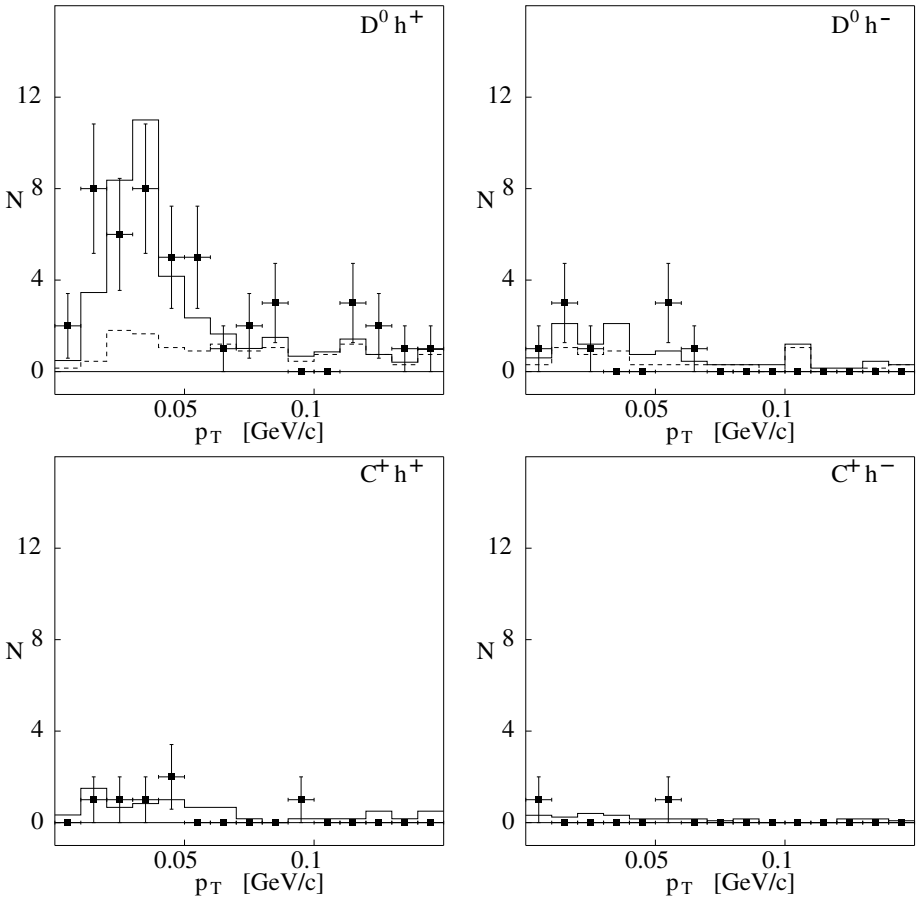

Figure 5.3: The number of charged hadron tracks (N) from the primary vertex as function of the transverse-momentum (p_T). The panel in the left (right) upper corner shows the p_T of positively (negatively) charged hadrons with respect to the D^0 direction. The panel in the left (right) lower corner shows the p_T for positively (negatively) charged hadrons with respect to direction of positively charged charm particles. The meaning of the different points and curves is explained in the text.

5.5 Efficiency and background evaluation

The detection efficiencies and expected background contamination were evaluated with a detailed Monte-Carlo simulation of the experiment based on the GEANT3 simulation framework [264]. The GEANT3 framework was also used for the modelling of the neutrino beam. A large number of deep-inelastic neutrino interactions were generated according to the beam spectrum by the JETTA generator [265] developed from LEPTO [266] and JETSET [267]. The simulated response of the detectors was processed through the standard chain of reconstruction programs. The efficiency of the event location and reconstruction in the emulsion was obtained by a detailed simulation of the efficiency and resolution of the net-scan procedure. In order to simulate realistic conditions of background grains in the emulsion, the data of empty volumes, i.e. net-scan volumes where no neutrino interaction is present, were overlaid on the simulated events.

5.5.1 Background evaluation

The main source of background is due to π^+ tracks from the primary vertex in events with a D^0 which have a p_T with respect to the D^0 in the signal region as defined in section 5.4. The number of background events in the signal region was estimated using D^0 events from the Monte-Carlo simulation, excluding the events coming from D^{*+} production. The simulated p_T distribution in the $\pi^+ + D^0$ channel was then normalized by comparing the number of events observed in the region $p_T < 0.1\,\mathrm{GeV}/c$ in the $\pi^- + D^0$ channel with the data in that channel. The total background was found to be $4.9 \pm 1.6(\mathrm{stat}) \pm 1.0(\mathrm{syst})$. The statistical error comes mainly from the normalization with respect to the events with a π^- (or other negative hadron). The systematic error is an estimate of the accuracy of the simulation.

Within the statistical accuracy, the simulated background agrees well with the events observed in the combination of a D^0 with a negative hadron, and for events with charged charm particles combined with positive and negative hadrons, respectively. Only in the channel with a D^0 and a positive hadron, is a clear excess of events above the predicted background observed. The p_T distribution of the excess is compatible with the simulated detector response.

The background to the sample of D^0 events coming from neutral strange particle decays such as Λ^0 and K^0_S is negligible due to the much longer decay length of these particles. Their number has been evaluated for the four emulsion stacks and found to be 11.5 ± 1.9 Λ^0's and 25.1 ± 2.9 K^0_S's in the full D^0 sample, respectively [268]. Since the calculation of the background coming from randomly associated positive hadrons from the primary vertex in combination with a D^0 has been normalized to the number of negative hadrons with the same kinematic properties, the random associations of a neutral strange particle with a π^+ have been taken into account implicitly. Their number can be estimated to give approximately $0.3 \cdot 10^{-3}$ events in the signal region. A potentially larger background is caused by K^* decays into a K^0_S and a π^+. With the assumption that all K^0_S's originate from K^* decay, 0.3 ± 0.1 events would pass the selection criteria. This estimate can thus be regarded as an upper limit for this background.

5.5.2 Detection efficiency

Since only the ratio of D^{*+} events with respect to the D^0 events is considered, only the efficiency associated with the detection of the π^+ has to be considered. Any energy-dependent effect in distinguishing the D^0 from D^{*+} decay from other D^0's, which would spoil the cancellation of the efficiency is very small and is included in the simulation. The efficiencies in locating events of the two types in the emulsion are expected to be equal to a high accuracy.

The important issues related to the π^+ detection are the efficiency in attaching the π^+ to the primary vertex in the reconstruction, the efficiency in measuring its momentum, and the ability of the Monte-Carlo chain to simulate the p and p_T resolution correctly. The combined systematic uncertainty in the product of the efficiency to find the π^+ and in the efficiency in measuring its momentum was estimated to be 7 %. Such a value is obtained by observing the differences in the fraction of tracks with a measured momentum predicted by the simulation and observed in the data for different track samples. The samples compared were the tracks from primary neutrino vertices with those from D^0 decays. The efficiency in finding the π^+ track at the primary vertex is well reproduced by the simulation, and the uncertainty in this calculation contributes to a smaller extent to the systematic error.

A study of the effects governing the p_T resolution shows that the most critical ingredient is the measurement of the angle of the D^0. From a comparison of measurements using the vertex reconstruction with the tracks found in the net-scan procedure and the vertex measurement in the manual scanning process, an angular resolution of 10 mrad is deduced at short flight paths and 5 mrad at long flight lengths. Using these numbers a 5 % uncertainty in the efficiency of the cut in p_T is evaluated.

The overall uncertainty in the efficiency is 11 %, which includes the systematic uncertainty in the efficiency in measuring the π^+ momentum, the uncertainty in the effect of the p_T cut and the statistical error of the simulation.

5.6 Results and conclusion

There are 27 events with a positive hadron in the signal region in the D^0 sample. Using the evaluation of the background as described in section 5.5.1 amounting to 4.9 ± 1.9, a signal of 22.1 ± 5.5 events is obtained.

The most direct measurement which can be obtained is the ratio of D^{*+} and D^0 production in charged-current neutrino interactions. This ratio can be expressed as:

$$\frac{\sigma(D^{*+})}{\sigma(D^0)} = \frac{N(D^{*+} \to D^0\,\pi^+)}{N(D^0)} \cdot \frac{\epsilon(D^0)}{\epsilon(D^{*+} \to D^0\,\pi^+)} \cdot \frac{1}{B(D^{*+} \to D^0\,\pi^+)} \quad ,$$

where $N(D^{*+} \to D^0\,\pi^+)$ and $N(D^0)$ are the number of D^{*+} and D^0 events observed, respectively, and $\epsilon(D^{*+} \to D^0\,\pi^+)$ and $\epsilon(D^0)$ their relative detection efficiencies. The ratio of these efficiencies is 0.176 ± 0.020. The branching ratio $B(D^{*+} \to D^0\,\pi^+)$ is 0.677 ± 0.005. Substituting the numerical values, one obtains:

$$\frac{\sigma(D^{*+})}{\sigma(D^0)} = 0.38 \pm 0.09(\text{stat}) \pm 0.05(\text{syst}) \quad . \tag{5.2}$$

Under the assumption that the D^{*0} and D^{*+} production rates are equal and recalling that the D^{*0} always decays into a D^0, it can be concluded that most D^0's in neutrino interactions are produced through the decay of a D^*:

$$\sigma(D^* \to D^0) \,/\, \sigma(D^0) = 0.63 \pm 0.17 \quad .$$

Following Ref. 269 and defining R_2 as the fraction of D^0's coming from D^{*+} decays, one obtains $R_2 = 0.25 \pm 0.10$ where the statistical and systematic errors are combined. With the definition $f_V = V \,/\, (P+V)$, the ratio of the vector D meson production and the sum of vector and pseudoscalar production of D mesons as introduced in Ref. 269, one finds $f_V = 0.51 \pm 0.18$. Within the precision, this determination is consistent with the value for the ratio of vector meson and pseudoscalar meson production (three to one) expected from simple spin arguments and with more precise measurements in $e^+\,e^-$, $\pi\,\mathrm{N}$ and $\gamma\,\mathrm{N}$ experiments [270].

The rate of D^{*+} meson production relative to the neutrino charged-current interaction cross-section can be obtained by combining the result in equation (5.2) with the measurement $\sigma(D^0) \,/\, \sigma(\mathrm{CC}) \;=\; [2.69 \pm 0.18 \pm 0.13]\,\%$ obtained using the same D^0 sample [263].[1] One then obtains:

$$\frac{\sigma(D^{*+})}{\sigma(CC)} \;=\; [1.02 \pm 0.25(\mathrm{stat}) \pm 0.15(\mathrm{syst})]\;\% \quad .$$

The NOMAD experiment [259], operating in the same neutrino beam as CHORUS, has reported the rate of D^{*+} production per charged-current neutrino interaction to be $[0.79 \pm 0.17(\mathrm{stat}) \pm 0.10(\mathrm{syst})]\,\%$. The BEBC bubble chamber data [257] were reanalysed combining several datasets using a neutrino beam with energies similar to CHORUS. This group reported the rate of D^{*+} production per charged-current neutrino interaction to be $[1.22 \pm 0.25]\,\%$. Our result is consistent with these measurements. At the higher energies of the Tevatron beam a value of $[5.6 \pm 1.8]\,\%$ has been found [258].

[1] The D^0 production rate had been obtained using only the four-prong decay topology for which practically all decay modes are available in the literature. This procedure minimizes the systematic error due to the unmeasured decay modes in the two-prong topology and the decay modes into final states with neutral particles only.